

NASA TM X-65911

65911

IONOSPHERE TOTAL ELECTRON MEASUREMENTS AS EXTRACTED FROM SATELLITE TRACKING DATA

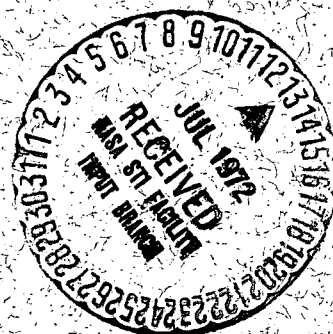
(NASA-TM-X-65911) IONOSPHERE TOTAL
ELECTRON MEASUREMENTS AS EXTRACTED FROM
SATELLITE TRACKING DATA C.W. Murray, Jr.,
et al (NASA) 21 Jun. 1972 19 p CSCL 04A

N72-26310

Unclas
G3/13 33639

CHARLES W. MURRAY, JR.
P. E. SCHMID
S. RANGASWAMY

JUNE 21, 1972



The logo for Goddard Space Flight Center, consisting of the letters "GSFC" in a bold, sans-serif font inside a black circle.

— GODDARD SPACE FLIGHT CENTER —
GREENBELT, MARYLAND

X-551-71-475
Preprint

IONOSPHERE TOTAL ELECTRON MEASUREMENTS
AS EXTRACTED FROM SATELLITE TRACKING DATA

Charles W. Murray, Jr.
P. E. Schmid
NASA, Goddard Space Flight Center

S. Rangaswamy
National Academy of Science

June 21, 1972

GODDARD SPACE FLIGHT CENTER
Greenbelt, Maryland

IONOSPHERE TOTAL ELECTRON MEASUREMENTS AS EXTRACTED FROM SATELLITE TRACKING DATA

ABSTRACT

The Goddard Range and Range Rate System (GRARR) determines the range of a spacecraft by measuring the group delay of a modulated wave and the range rate by measuring the Doppler phase shift of the carrier. Therefore, it has an inherent capability to determine the ionospheric dispersive propagation effects on the tracking signals which are of equal magnitude but opposite sign for the range and range rate measurements. In this paper an analytical technique to obtain corrections and the equivalent total electron content along the vertical using VHF GRARR data and a radial model of the ionosphere is presented. The results of computation for a representative pass is given, and an estimated accuracy is discussed from a statistical view point. Using GRARR range, range rate and angle tracking data from Explorer 41 (also termed Interplanetary Monitoring Platform - G) values of total electron content on the order of $10^{17} - 10^{18}$ (electrons/meter²) have been obtained. These values are seen to be in good agreement with estimates of the total electron content from ionospheric profiles using f_oF_2 predict data.

CONTENTS

	Page
ABSTRACT	ii
INTRODUCTION	1
ANALYSIS	4
EXPERIMENTAL RESULTS	8
CONCLUSIONS	9
REFERENCES	10

LIST OF FIGURES

Figure 1. Goddard Range and Range Rate Measuring System	12
Figure 2. Orbital Characteristics of Explorer 41 (IMP-G)	12
Figure 3. Ionospheric Geometry	14
Figure 4. Spacecraft Tracking Ionosphere Biases for 1000 km Altitude Overhead Pass	15
Figure 5. Example of Integrated Content Predicted Versus Observed	16

ANALYAI

IONOSPHERE TOTAL ELECTRON MEASUREMENTS AS EXTRACTED FROM SATELLITE TRACKING DATA

INTRODUCTION

Demands for accurately locating and predicting the positions of satellites, in determining continental drift and polar motion, earthquake prediction, and geodesy in general, impose stringent requirements for correcting spacecraft tracking data for the effects of known physical phenomena.

The interpretation of radio tracking signals will lead to a bias in range and range rate calculated from these data if a free-space velocity (i.e., the velocity of light in a vacuum) is assumed for the radio signals. This propagation bias which is due to the ionospheric plasma is directly proportional to the number of electrons along the ray path connecting the satellite and the tracking station.

The NASA Goddard Range and Range Rate tracking system is used in two frequency bands, namely VHF (~140 MHz) and S-Band (~2 GHz). The VHF system is ideal for both probing the ionosphere as well as verifying ionospheric models which can then be applied to the inherently more accurate S-Band system. In the Goddard Range and Range Rate System ranging is accomplished by the use of ranging sidetones. The sum of the ranging sidetones phase-modulates the uplink signal from the tracking station and the uplink signal in turn phase-modulates the downlink signal from the satellite. The phase shift between the ground-transmitted sidetones and the satellite transponder-returned sidetones is used

as the basic measure of two-way range between the tracking antenna and satellite. The range rate measurement consists of the time in seconds required to count a fixed number of cycles of the difference frequency between the received and transmitted frequency plus a fixed frequency offset. This fixed frequency offset, phase locked to the system reference oscillator permits Doppler sign determination and is removed during the data processing. The data as shown in Figure 1 is consequently a measure of the total change in frequency in the round trip of the signal from the ground station through the satellite transponder and back (reference 1).

It can be shown from magneto-ionic theory that the ionosphere causes a time delay of the sidetone ranging signal and a doppler phase advance of the carrier signal. In the GRARR backing system the time delay and phase advance respectively are given by:

$$\tau_1 = \frac{-2R_T}{c} - \frac{2K}{cf_{eq}^2} \quad (\text{group delay}) \quad (1)$$

$$\tau_2 = \frac{-2R_T}{c} + \frac{2K}{cf_{eq}^2} \quad (\text{Doppler phase advance}) \quad (2)$$

where R_T in the absence of calibration bias is the freespace (line of sight) range between the tracking station antenna and the satellite, c is the speed of light, $1/f_{eq}^2$ is the arithmetic mean of the reciprocal uplink and downlink frequency squared and K is proportional to the total electron content along the ray path connecting the satellite and the ground station. As will be shown, any range calibration bias is removed by differentiation.

Also:

$$K = \frac{40.3I_v}{\sin E} \quad (\text{MKS})$$

$$I_v = \text{electron/meter}^2$$

$$f_{eq} = 141 \times 10^6 \text{ Hz}$$

$$c = (2.997925)10^8 \text{ meters/second}$$

The purpose of this paper is to show the effect of the ionosphere upon the range and range rate biases in these two data types and to extract the total electron content from GRARR VHF range, range rate, and angle measurements using the time derivatives of equations (1) and (2).

The analysis in this paper is carried out for the Goddard Range and Range Rate VHF tracking data taken from Explorer 41 (IMP-G), a spin stabilized satellite launched 21 June 1969 in eccentric orbit about the earth (see Figure 2) and having the following approximate orbital characteristics.

Semi-major axis	95000 km
Argument of perigee	203°
Eccentricity	0.9
Right Ascension of the Ascending Node	104°
Inclination	85°

The perigee radius of IMP-G is approximately 9500 km (perigee height of 3122 km), the apogee radius 180,500 km (apogee height of 174,122 km), and the period is 3.4 days.

ANALYSIS

Rewriting equations (1) and (2)

$$\tau_1 = \frac{-2R_T}{c} - \frac{2K}{cf_{eq}^2} \quad (1)$$

$$\tau_2 = \frac{-2R_T}{c} + \frac{2K}{cf_{eq}^2} \quad (2)$$

where R_T is the true freespace (line of sight) range between the tracking station antenna and the satellite, c is the freespace speed of light, $\frac{1}{f_{eq}^2}$ is the arithmetic mean of the reciprocal of the uplink and downlink frequencies squared for the GRARR VHF transmission, i.e.,

$$\frac{1}{f_{eq}^2} = \frac{1}{2} \left[\frac{1}{f_t^2} + \frac{1}{f_{dn}^2} \right]$$

and K is proportional to the total electron content along the line of sight and is given by

$$K = \int_0^{R_T} \mu ds$$

$$\mu = \left(1 - \frac{N_e e^2}{\epsilon_o m \omega^2} \right)$$

where

- N_e = electron density = electrons/meter³
- e = electron charge = 1.602×10^{-19} coulombs
- m = electron mass = 9.11×10^{-31} kilograms
- ϵ_o = free space dielectric constant = 8.855×10^{-12} farad/meter
- ω = angular frequency = radians/second

Differentiating (1) and (2) and converting to range rate by (reference (2))

$$\dot{r} = \frac{-c\dot{\phi}}{\dot{\phi} + 2\omega} \doteq \frac{-c\dot{\phi}}{2\omega}$$

where $\dot{\phi}$ = the angular rate of change of phase (doppler) at the transmit (or side-tone) angular frequency.

For VHF satellites which are spin stabilized, the bias in the range rate k_{sp} (reference 3) due to the effect of the spin must be added

$$\dot{R} = \dot{R}_T + \left(\frac{1}{f_{eq}^2} \right) \left(\frac{dk}{dt} \right) \quad (3)$$

$$\dot{r} = \dot{R}_T - \left(\frac{1}{f_{eq}^2} \right) \left(\frac{dk}{dt} \right) + k_{sp} \quad (4)$$

where \dot{R} represents the differentiated range from the sidetone ranging system to be distinguished from \dot{r} which refers to a measurement from the range rate system.

For short data arcs K can be considered a function of the local elevation angle E at the approximate height h which is the height of the peak electron density of the ionospheric F_2 layer.

$$\frac{dK}{dt} = \frac{dK}{dE} \cdot \frac{dE}{dt} \quad (5)$$

Using a spherically symmetric model for the ionosphere in which the gradient is in the radial direction only we can write (see Figure 3),

$$K = \frac{40.3 I_v}{\sin E} \quad (6)$$

where I_v is the total electron content along the vertical at the point where the line of sight intersects the circle of radius $a + h$

$$\frac{dK}{dt} = - \left(\frac{\cos E}{\sin^2 E} \right) (40.3) I_v \frac{dE}{dt} \quad (7)$$

where E and $\frac{dE}{dt}$ are related to the ground elevation angle E' and ground elevation angle rate $\frac{dE'}{dt}$ by

$$E = \cos^{-1} \left(\frac{a}{a+h} \cos E' \right)$$

$$\frac{dE}{dt} = \left[1 - \left(\frac{a}{a+h} \right)^2 \cos^2 E' \right]^{-1/2} \left(\sin E' \right) \left(\frac{a}{a+h} \right) \left(\frac{dE'}{dt} \right)$$

From (3), (4), and (7) we can write an expression for I_v as a function of \dot{R} , \dot{r} , E and \dot{E} .

$$I_v = (\dot{r} - \dot{R} - k_{sp})(1/2) f_{eq}^2 \left(\frac{1}{40.3} \right) \left(\frac{\sin^2 E}{\cos E} \right) \left(\frac{1}{\dot{E}} \right) \quad (8)$$

This is the basic equation for the determination of I_v from range, range rate, and angle tracking data used in this analysis. Substituting I_v in (3) and (4) we obtain expressions for the biases in range and range rate due to the ionosphere.

$$\Delta R = \left(\frac{1}{f_{eq}^2} \right) \left(\frac{40.3 I_v}{\sin E} \right) \quad (9)$$

$$\Delta \dot{r} = \left(\frac{1}{f_{eq}^2} \right) \left(\frac{\cos E}{\sin^2 E} \right) (40.3) I_v \cdot \dot{E} \quad (10)$$

For purposes of calculation, the raw range, range rate, and elevation angle data was first smoothed by least squares polynomials and then the midpoints of the polynomials and differentiated polynomials used for values of \dot{R} , \dot{r} , E , and \dot{E} in (8), (9), and (10).

It should be noted that the ionospheric corrections to the range and range rate data are the negatives of (9) and (10).

Assuming a daytime value for I_v of 4×10^{17} electrons/m² and a satellite passing overhead in a 1000 km circular orbit and a VHF frequency of $f_{eq} = 141 \times 10^6$ Hz we can plot $\Delta\dot{R}$ and $\Delta\dot{r}$ as a function of the ground elevation angle E' . This is shown in Figure 4. It can be seen that an appreciable bias results in both data types. The VHF GRARR system at a 4 per second sample rate has a range rate resolution of better than 0.2 meters/second. With the 20 KHz sidetone the range resolution is on the order of 5 to 10 meters depending on the Doppler rate.

THE PREDICTED UNCERTAINTY OF I_v

Letting $\Delta\dot{R}$, $\Delta\dot{r}$, ΔE , and $\Delta\dot{E}$ represent errors in \dot{R} , \dot{r} , E , and \dot{E} , we can write an error ΔI_v in I_v from (8).

$$\Delta I_v = I_v(\dot{R} + \Delta\dot{R}, \dot{r} + \Delta\dot{r}, E + \Delta E, \dot{E} + \Delta\dot{E}) - I_v(\dot{R}, \dot{r}, E, \dot{E}) \quad (11)$$

or expanding in a Taylor series and retaining only first order partial derivatives

$$\Delta I_v = \left(\frac{\partial I_v}{\partial \dot{R}}\right) \Delta\dot{R} + \left(\frac{\partial I_v}{\partial \dot{r}}\right) \Delta\dot{r} + \left(\frac{\partial I_v}{\partial E}\right) \Delta E + \left(\frac{\partial I_v}{\partial \dot{E}}\right) \Delta\dot{E} \quad (12)$$

From (12) we can write an expression for the variance of I_v or $\sigma_{I_v}^2$ as

$$\sigma_{I_v}^2 = \left(\frac{\partial I_v}{\partial \dot{R}}\right)_M^2 \sigma_{\dot{R}}^2 + \left(\frac{\partial I_v}{\partial \dot{r}}\right)_M^2 \sigma_{\dot{r}}^2 + \left(\frac{\partial I_v}{\partial E}\right)_M^2 \sigma_E^2 + \left(\frac{\partial I_v}{\partial \dot{E}}\right)_M^2 \sigma_{\dot{E}}^2 + \left(\frac{\partial I_v}{\partial E}\right)_M \left(\frac{\partial I_v}{\partial \dot{E}}\right)_M \sigma_{\dot{E}E}$$

where $\sigma_{\dot{R}}^2$, $\sigma_{\dot{r}}^2$, σ_E^2 and $\sigma_{\dot{E}}^2$ are the variances of \dot{R} , \dot{r} , E , and \dot{E} respectively, and $\sigma_{\dot{E}E}$ is the covariance between E and \dot{E} . It should be noted that each of the partial

derivatives is evaluated at some nominal point M , usually taken at the midpoint of the data arc.

EXPERIMENTAL RESULTS

Goddard Range and Range Rate VHF tracking data taken from Explorer 41 (IMP-G) on October 6, 1971 at Carnarvon, Australia was analyzed. Using equation 8, the total electron content along the vertical was calculated for four data arcs. The results can be seen in Table 1 and Figure 5. It can be seen that there is excellent agreement between the observed and predicted values. A second degree least squares polynomial was used to smooth the range data, and a straight line was used to smooth the range rate data. The sampling rate was four per second and for the four data arcs approximately 200 points of range and range rate data were analyzed. The estimated standard deviation is shown along with the predicted value (with an uncertainty of approximately 10% for the local times indicated) which was obtained by a NASA/GSFC ionospheric model developed by examining tens of thousands of topside and bottomside profiles and presented at the 14th meeting of COSPAR, Seattle, June 1971 by R. B. Bent of DBA Systems, Inc., of Melbourne, Florida (reference 4).

CONCLUSIONS

In this paper it has been demonstrated that the Goddard Range and Range Rate System has an inherent capability for obtaining the total electron content along the ray path connecting the ground tracking station and the satellite. (From the determination of the total electron content, corrections can be made to raw range and range rate tracking data). These corrections are possible since the GRARR system makes independent measurements of group delay (range data) and Doppler phase shift (range rate data). This technique is a new one for the measurement of total electron content in that it combines both group and phase delays. The correction of raw range and range rate data is important in that more precise orbit determinations are possible and estimation of parameters such as continental drift, polar motion, etc., by regression analysis techniques can be made.

REFERENCES

1. Kronmiller, G., Jr., and Baghdady, E., "The Goddard Range And Range Rate System: Concept, Design, and Performance," NASA (GSFC) Report X-531-65-403, October 1965.
2. Kruger, B., "The Doppler Equation in Range and Range Rate Measurements", NASA (GSFC) X-507-65-385, 8 October 1965.
3. Marini, J. W., "The Effect of Satellite Spin On Two-Way Doppler Range Rate Measurements", NASA (GSFC), X-551-69-104, March 1969.
4. Bent, R. B., Llewellyn, S. K., and Schmid, P. E., "Ionospheric Refraction Corrections In Satellite Tracking", presented at the XIVth meeting of COSPAR, Seattle, Washington, June 1971.

Table I

Experimental Results

Local Time h m s	Number of Measurements Range and Range Rate	Observed $I_v \times 10^{-17}$ e/m ²	One Sigma $\times 10^{-17}$ e/m ²	Predicted $I_v \times 10^{-17}$ e/m ²
7 36 42	200	.99	.13	1.19
7 37 32	200	1.24	.19	1.21
7 38 22	200	.82	.16	1.21
7 40 2.5	204	.80	.10	1.26

Carnarvon, Australia
6 October 1971
Sampling rate 4/second
VHF Goddard Range
And Range Rate.

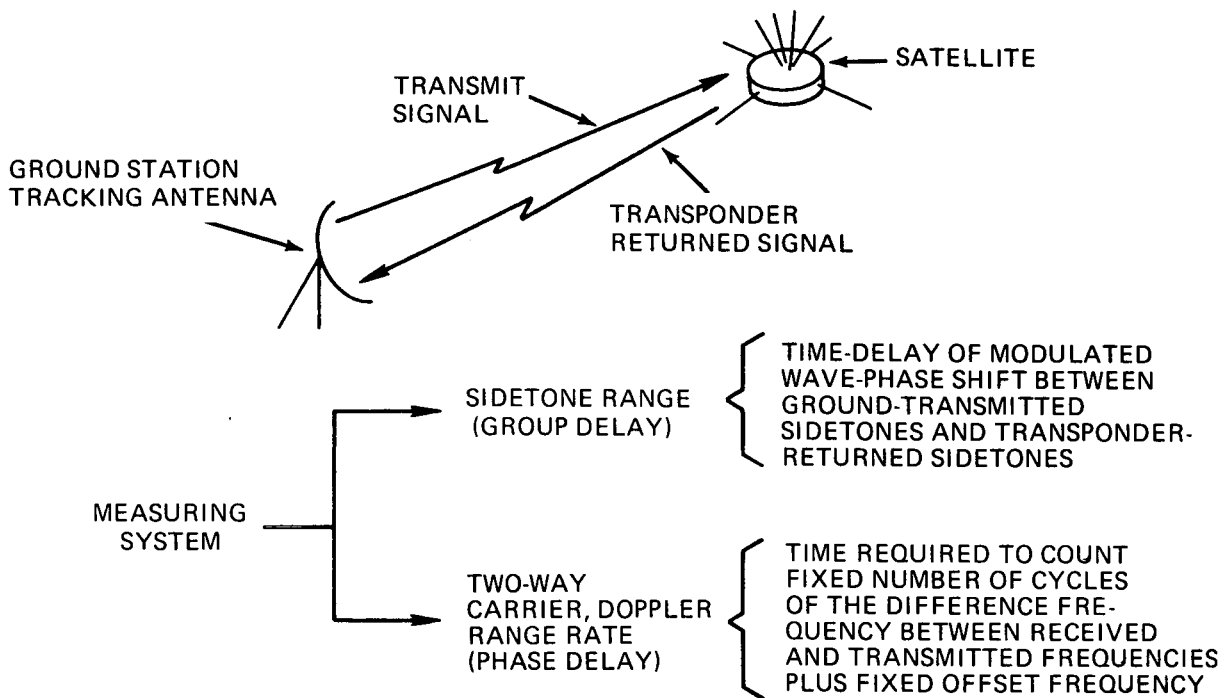
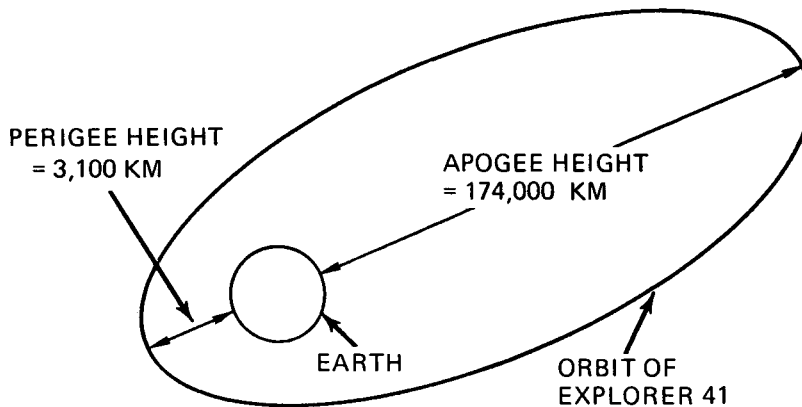


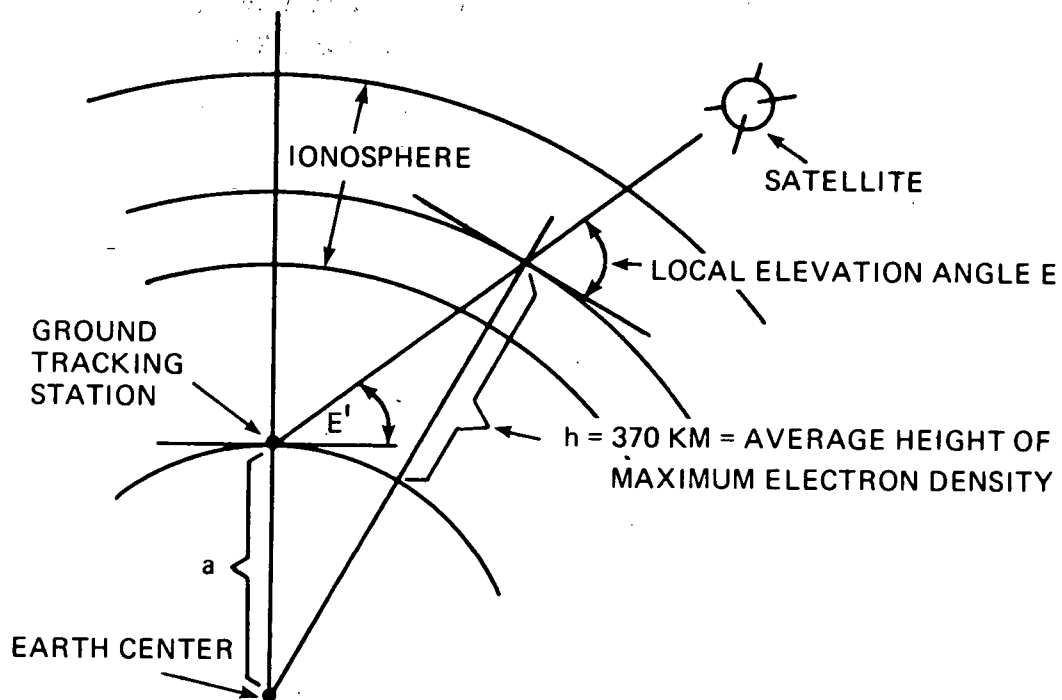
Figure 1. Goddard Range and Range Rate Measuring System



ORBITAL PARAMETERS

SEMI-MAJOR AXIS	9500 KM
ARGUMENT OF PERIGEE	203°
ECCENTRICITY	0.9
RIGHT ASCENSION OF ASCENDING NODE	104°
INCLINATION	85°
PERIOD	3.4 DAYS
LAUNCH DATE	21 JUNE 1969

Figure 2. Orbital Characteristics of Explorer 41 (IMP-G)



$$E = \cos^{-1} \left[\frac{a}{a+h} \cos E' \right]$$

$$\dot{E} = \left[1 - \left(\frac{a}{a+h} \right)^2 \cos^2 E' \right]^{-1/2} \left[\sin E' \right] \left[\frac{a}{a+h} \right] \dot{E}'$$

$$I = \frac{I_v}{\sin E}$$

Figure 3. Ionospheric Geometry

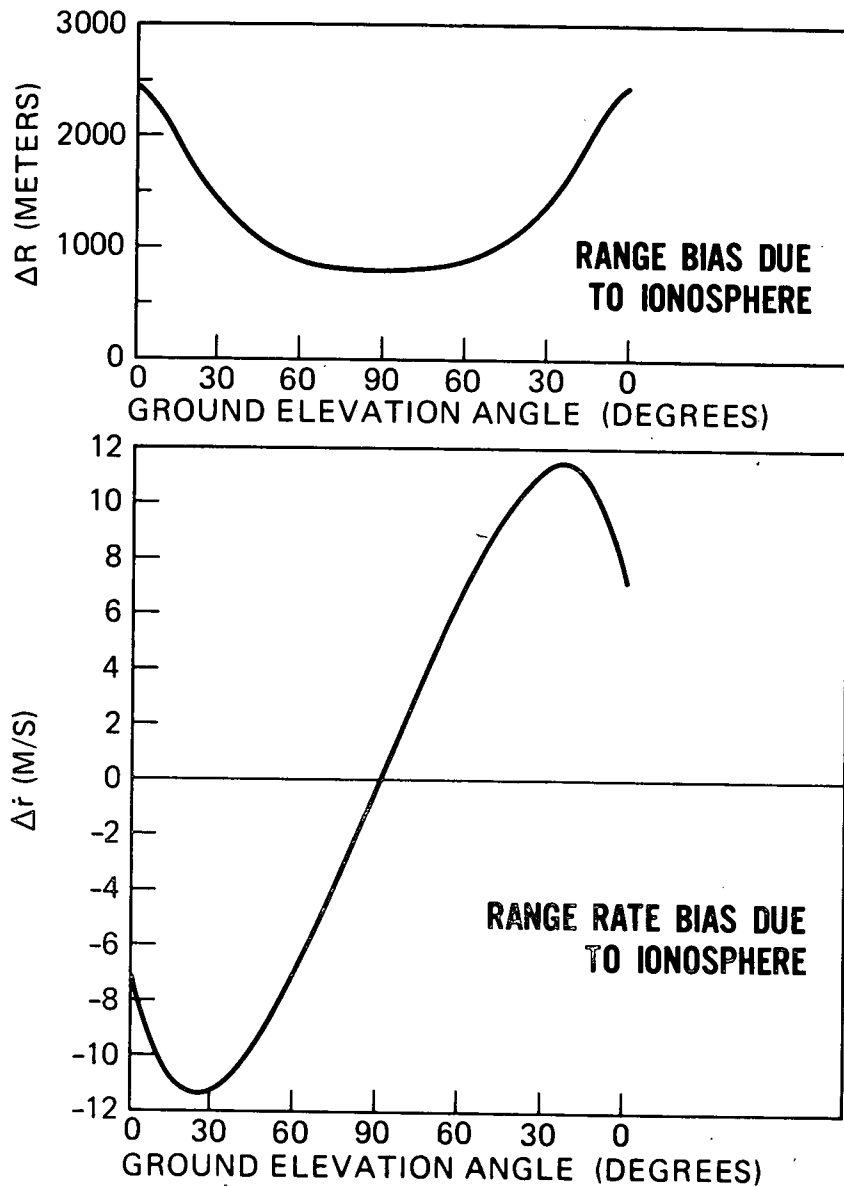


Figure 4. Spacecraft Tracking Ionosphere Biases for 1000 km Altitude Overhead Pass

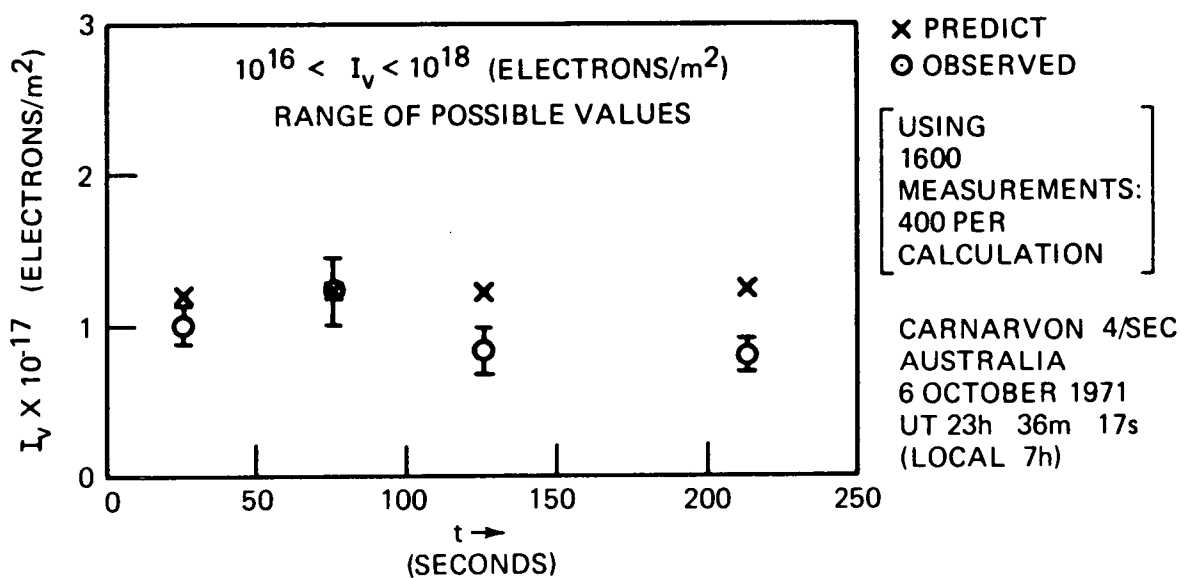


Figure 5. Example of Integrated Content Predicted Versus Observed.